PROCEEDINGS OF THE ROYAL SOCIETY B

Proc. R. Soc. B (2010) **277**, 1161–1168
doi:10.1098/rspb.2009.1980
Published online 16 December 2009

Selective biodegradation of keratin matrix in feather rachis reveals classic bioengineering

Theagarten Lingham-Soliar[1,*], Richard H. C. Bonser[3] and James Wesley-Smith[2]

[1]*Biological and Conservation Sciences, and* [2]*EM Unit, University of KwaZulu-Natal, P. Bag X54001, Durban 4000, South Africa*
[3]*School of Construction Management and Engineering, University of Reading, Reading, UK*

Flight necessitates that the feather rachis is extremely tough and light. Yet, the crucial filamentous hierarchy of the rachis is unknown—study hindered by the tight chemical bonding between the filaments and matrix. We used novel microbial biodegradation to delineate the fibres of the rachidial cortex *in situ*. It revealed the thickest keratin filaments known to date (factor >10), approximately 6 μm thick, extending predominantly axially but with a small outer circumferential component. Near-periodic thickened nodes of the fibres are staggered with those in adjacent fibres in two- and three-dimensional planes, creating a fibre–matrix texture with high attributes for crack stopping and resistance to transverse cutting. Close association of the fibre layer with the underlying 'spongy' medulloid pith indicates the potential for higher buckling loads and greater elastic recoil. Strikingly, the fibres are similar in dimensions and form to the free filaments of the feather vane and plumulaceous and embryonic down, the syncitial barbules, but, identified for the first time in 140+ years of study in a new location—as a major structural component of the rachis. Early in feather evolution, syncitial barbules were consolidated in a robust central rachis, definitively characterizing the avian lineage of keratin.

Keywords: feather rachis; matrix biodegradation; fibres/syncitial barbules; biomechanics; evolution

1. INTRODUCTION

The feather is an extraordinary device and among the most prominent of a series of adaptations that facilitates flight in birds. The main structural support is the rachis, which is symmetrically located in contour feathers but nearer the leading edge (asymmetrical) in flight feathers. The cortex of the feather comprises the bulk of the material of the rachis and has been shown to account for most of its tensile strength (Purslow & Vincent 1978). It is constructed of compact β keratin, the keratin of reptiles and birds (sauropsids), a light, rigid material (Fraser & Parry 2008). However, besides the fine microfibrils and fibrils of the rachis (Filshie & Rogers 1962), we know little of the gross keratin fibrous structure of the rachis and consequently of how it contributes to extreme mechanical strength and flexibility.

Absence of structural data in feather keratin is undoubtedly a consequence of the tight bond between the polymeric filaments of keratin and the amorphous polymer matrix (Filshie & Rogers 1962; Rudall 1968). Attempts to section and freeze-fracture the rachidial cortex in feathers to reveal higher structural organization have proved unsuccessful (analogous to physically trying to recover individual matchsticks after they had been super-glued together into a bundle—sectioning would merely show the internal fibrils of the matchsticks). X-ray diffraction analysis has been useful with respect to molecular structure and fibril angles (Rudall 1968; Fraser *et al.* 1971) but has produced no data on gross hierarchical structure and morphology of the filaments.

The objective of our study was to obtain information on the filamentous structure of the feather rachis. We believed this would be a key to answers on feather biomechanics, namely how structure may contribute to extreme strength. However, in order to accomplish this, we had to find a means to get around the almost inextricable bonding between the filamentous and matrix texture of feather keratin. Although biodegradation of plant and animal tissue after maceration and or chemical extraction has become increasingly important over the past decade in industrial applications (Martínez-Hernández *et al.* 2005; Kersten & Cullen 2007; Ander & Eriksson 2008; Marcondes *et al.* 2008)—it had never been used as an investigative tool before. We use a natural microbial fauna for the first time in selective biodegradation in order to circumvent the limits of conventional structure-determination methods. Our strategy was simple and involved allowing the naturally occurring keratinophilic fungal genera in birds (Dixit & Kushwaha 1991; Deshmukh 2004; Kushwaha & Gupta 2004) to biodegrade the keratin matrix. We anticipated the possibility of selective biodegradation occurring on the basis of the two general classes of proteins present in keratin, a high-sulphur fraction of the amorphous matrix (derived from the sulphur–sulphur cross-links that keep the fibres intact) and a low sulphur fraction of the microfibrillar component. Although these fractions were determined

* Author for correspondence (linghamst@ukzn.ac.za).

Electronic supplementary material is available at http://dx.doi.org/10.1098/rspb.2009.1980 or via http://rspb.royalsocietypublishing.org.

Received 29 October 2009
Accepted 25 November 2009

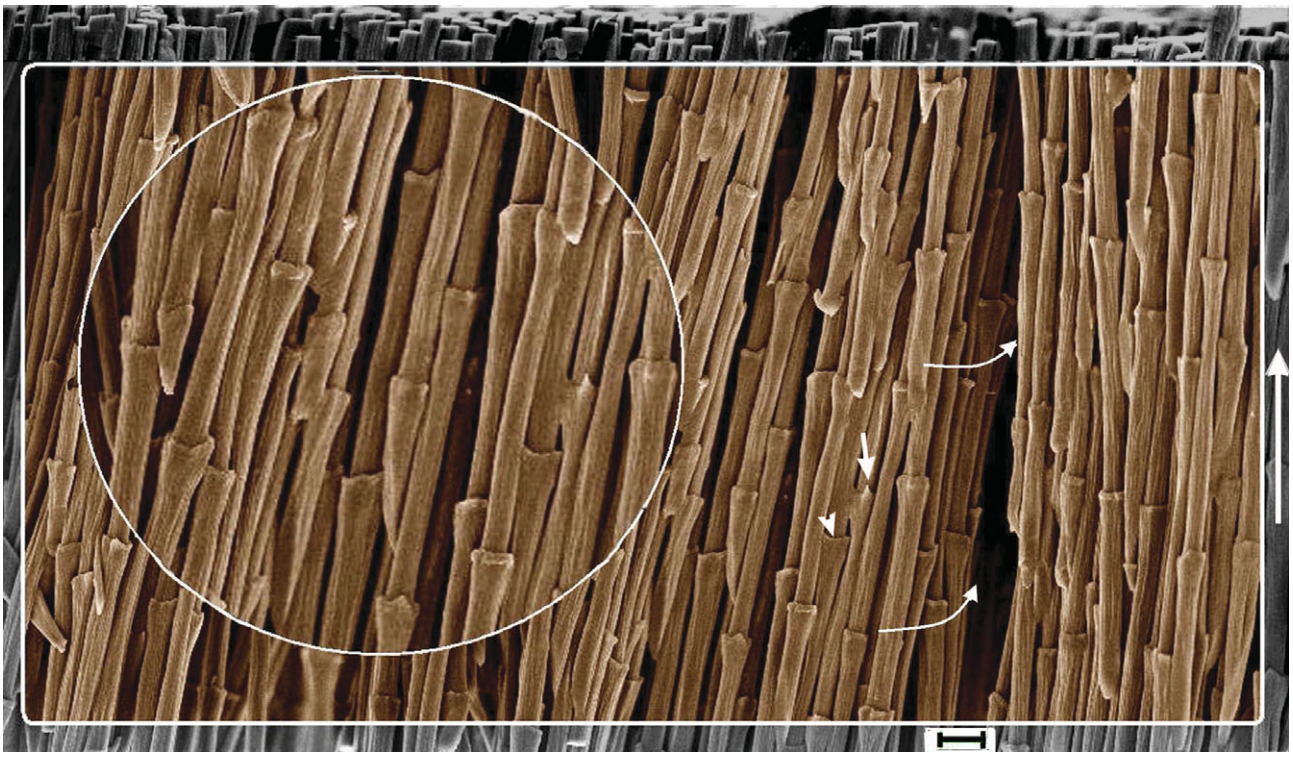

Figure 1. SEM of fibres (syncitial barbules) in the cortex of feather rachis of *Gallus gallus* exposed after fungal biodegradation of matrix (resin embedded and etched). All fibres show regularly spaced syncitial nodes that extend in the proximo-distal direction of the rachis (vertical arrow on the right). The syncitial nodes show variations in morphology, terminating in hooks (arrow; details in figure 2*a*) or a ring (arrowhead), while others are intermediate between the two. Fibres are densely packed through the cortex (curved arrow) and indicate that the nodes are staggered in arrangement on two- and three-dimensional planes. Inset, detail. Also see the electronic supplementary material, figures S1 and S2. Scale bar, 10 μm.

on α keratins (Alexander & Earland 1950; Gillespie *et al.* 1968; Lindley & Cranston 1974), we believed, as implied by some workers (Wainwright *et al.* 1976), that the fractions might be similar in β keratins. We mention in parentheses subsequent research (Eckhart *et al.* 2008) that shows that cysteine-rich α keratins are not restricted to mammals and that the evolution of mammalian hair may have involved the cooption of pre-existing structural proteins (lizards and birds) and, interestingly, that in the keratins in lizard claws there were sulphur–sulphur bonds unrelated to mammalian counterparts.

2. MATERIAL AND METHODS

(a) *Biodegradation of feathers*

Feathers were allowed to biodegrade on five domestic chickens, *Gallus gallus*, in the laboratory at normal room temperature (22–30°C) and humidity (50–70%) after removal of flesh underlying the skin as well as the internal organs (similar to taxidermy preparation). For the first few weeks, the specimens were placed in a fume cupboard provided with an intermittent extractor fan after which the fan was turned off. Feather biodegradation was slow. After the first year, the feathers along the wing bones, sternum, legs and back still looked in a good state besides discoloration. Examination of a selection of feathers by standard polarizing light microscopy (×1000; Zeiss Axiophot light microscope with differential interference contrast) showed few signs of structural degradation. After 18 months decomposition and over a further period of six months, feathers from the wing and breast areas were examined by scanning electron microscope (SEM) (LEO 1450).

(b) *rRNA analysis of fungi present on the delineated fibres*

Fungal hyphae and spores, evident in all biodegraded feather sections of *G. gallus*, were cultured. The recovered species of fungi were identified by rRNA sequence analysis (for complete details of material and methods, see the electronic supplementary material).

3. RESULTS

(a) *Morphology and structure of β-keratogenic tissues of the feather rachis*

Fungi preferentially degraded the amorphous keratin matrix. Selective biodegradation of the keratin matrix occurred in samples of feather rachis (indistinguishable between plumulaceous and flight feathers) through the entire depth of the rachidial cortex and left the 'fibres' cleanly exposed. SEM reveals for the first time densely packed, predominantly axially oriented filaments with an average diameter of approximately 6 μm, the thickest by far recorded in the structural elaboration of any form of keratin by a magnitude greater than 10 (figures 1 and 2, electronic supplementary material, figures S1 and S2). We also show for the first time SEM images of identical filaments circumferentially oriented in superficial layers of the cortex, approximately 15 per cent of the total depth of filaments in the cortex (figure 3). From a morphological and biomechanical perspective, both the axial and circumferential filaments are designated as fibres

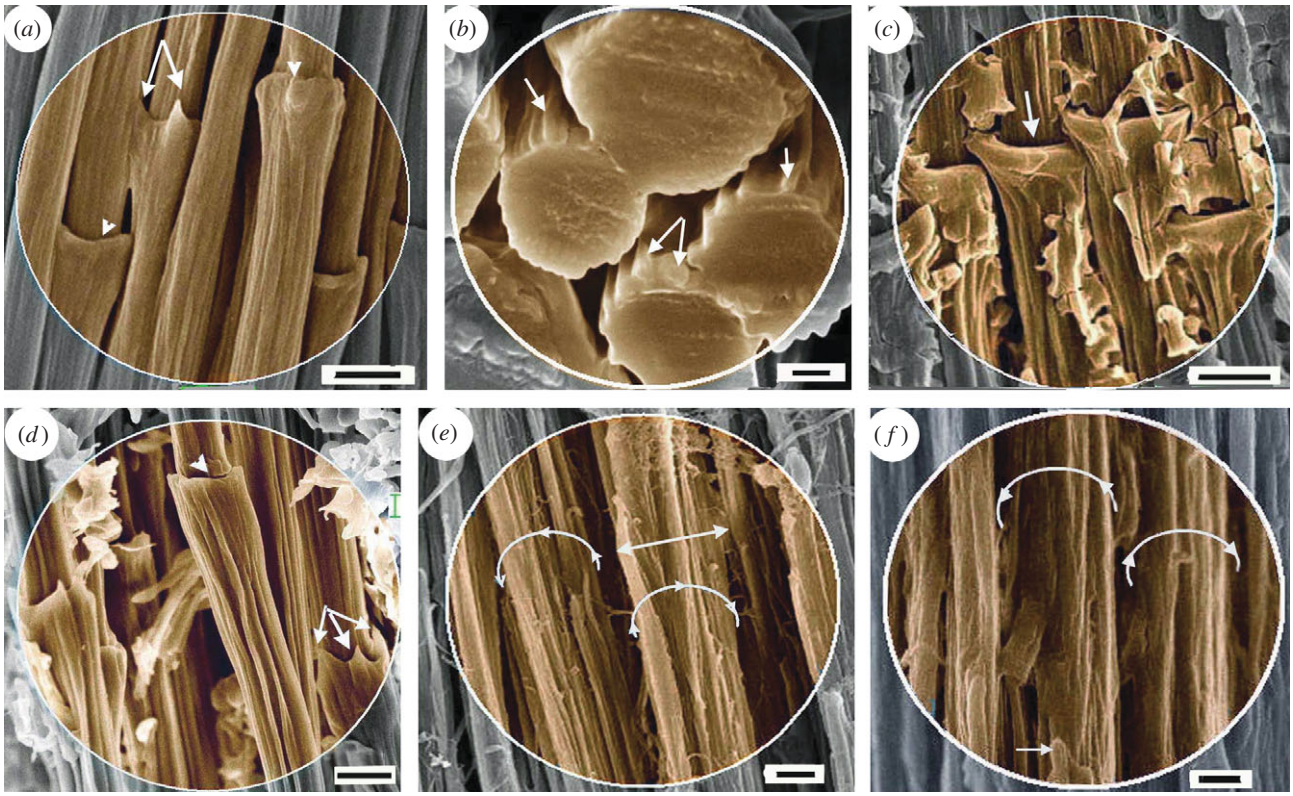

Figure 2. SEM of feather rachidial (cortex) fibres (syncitial barbules). (*a*,*b*) Biodegraded fibres of *Gallus gallus* (resin embedded and etched). (*a*) A detail showing fibres, syncitial nodes and macrofibrils; arrows and arrowheads show hooked and ringed terminations of nodes, respectively. (*b*) Group of fibres seen in cross section; the thicker cross sections indicate proximity to the syncitial nodes; arrows show macrofibrils. (*c*)–(*e*) Non-biodegraded rachidial fibres. (*c*) *Gallus gallus*, showing ringed nodes (arrow). (*d*) Fibres of *Falco tinnunculus* showing two morphologies of syncitial nodes, hook (arrows) and ring (arrowhead), and component macrofibrils. (*e*) Fibres of *Falco peregrinus*. The fibre surface is partially stripped, showing the component macrofibrils (diameter approx. 400–500 nm); part of the syncitial node remains (double-headed arrow). (*f*) Fibres of taxidermy specimen of *Falco biarmicus* (Durban Museum, dated 1966, accession no. 479) with matrix degraded and somewhat superficially degraded but intact fibres. (*a*,*c*,*d*) Scale bar, 5 μm; (*b*) 1 μm; (*e*,*f*) 2 μm.

(a specific term not to be used generally to mean filaments), which can be separated into thick fibrils or megafibrils down to the finest fibrils including the protofibrils. Macrofibrils, next down in the hierarchy of feather keratin, range in diameter from approximately 300–500 nm (figure 2; electronic supplementary material, figure S2*b*) (comparable to the thickest filaments noted in mammalian keratin; McKinnon 2006) and below them are fibrils approximately 100 nm thick (electronic supplementary material, figure S2*c*). Other authors mentioned here describe the finer fibrils.

The fine detail exposed by fungal biodegradation (seen graphically in figure 4*a*) has enabled observation of the most striking and highly unexpected feature of the fibres—nearly periodic nodes at intervals of approximately 70 μm along the entire length of each fibre (figure 1; electronic supplementary material, figure S1 and table S2). Each node terminates in hooks or as a ring (figures 1 and 2*a*,*d*, arrows and arrowheads, respectively). In both features, they resemble structures observed in embryonic and plumulaceous down filaments (Chandler 1916; Lucas & Stettenheim 1972) (figure 4*b*). The fibres also compare closely with down filaments in thickness, in subdivision of filaments into megafibrils (figures 2 and 4*b* (inset) and electronic supplementary material, figure S2*a*,*b*) and in spacing of the nodes along the filaments (electronic supplementary material, table S2). The nodes in adjacent fibres are staggered in both two- and three-dimensional planes.

The exquisite detail of the fibres seen after biodegradation of the matrix can perhaps be better appreciated when compared with a partially degraded part of the rachis (figure 3) where a substantial amount of the matrix was not biodegraded, presenting a graphic view of the fibre–matrix texture for the first time. Calculations from SEM images of 'holes' left in the matrix by the fibres (figure 3) reveal that they occupy 68.5 per cent of the keratin fibre–matrix texture (electronic supplementary material, material and methods), similar to the microfibrillar proportion suggested by chemical analysis of α keratin (Alexander & Earland 1950). In figure 5*a*, we present a schematic view of the fibres, in figure 5*b* the probable structures biodegraded in the amorphous matrix and in figure 5*c* approximate thickness of the structural components of the rachis.

Making comparisons with non-biodegraded feather rachises was obviously extremely difficult because of the tightly bonded filaments and matrix but was achieved through perseverance after numerous sections, if somewhat ragged, armed with our hindsight knowledge from the biodegradation experiments (see the electronic supplementary material, material and methods). A fibre diameter of approximately 6 μm was found to be rather constant in a number of bird species investigated

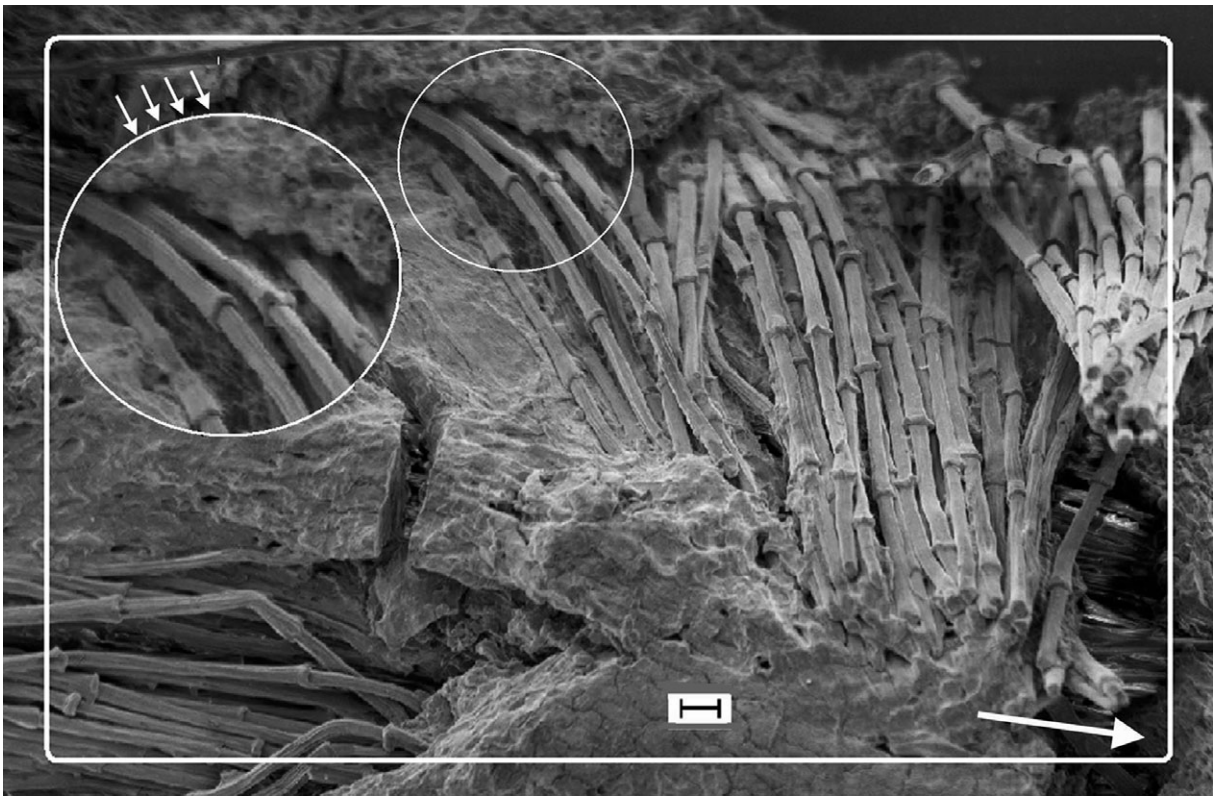

Figure 3. SEM of biodegraded feather rachis of *Gallus gallus* (resin embedded and etched). Circumferential fibres (syncitial barbules), identical to the longitudinal fibres (see below in the figure), wound round the outer 'layers' of the rachidial cortex. The matrix is partially degraded and shows the honeycomb-like structure in which the fibres are embedded in life (small arrows). Detail shows fibres, comparable to steel rebars in concrete (see text). Arrow shows long axis of rachis. Scale bar, 10 μm.

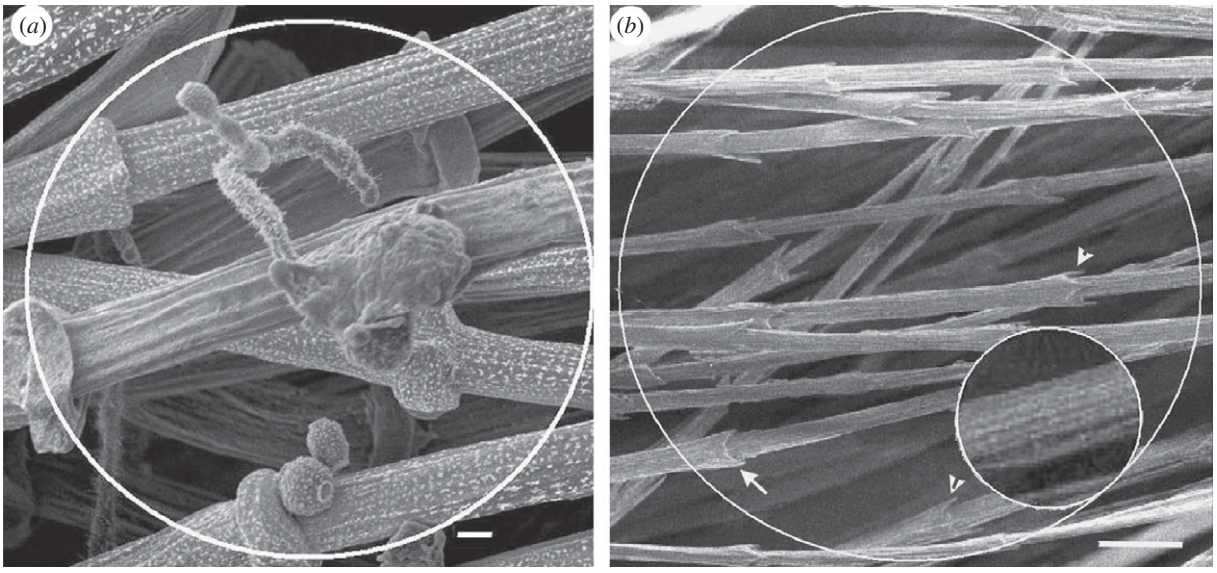

Figure 4. SEM of fibres (syncitial barbules). (*a*) *Gallus gallus*. Rachidial (cortex) fibres and fungal hyphae and spores (detail in the electronic supplementary material, figure S1). (*b*) Free syncitial barbules (similar to rachidial cortex fibres) from the downy part of a pennaceous feather of *Falco peregrinus*. Arrows show both ringed and hooked terminations of the syncitial nodes. Inset shows the megafibrils of the fibres (cf. figure 4*a* and electronic supplementary material, figure S2). (*a*) Scale bar, 2 μm and (*b*) 10 μm.

i.e. *G. gallus*, rock kestrel (*Falco tinnunculus*) (figure 2*c*,*d*, *respectively*; electronic supplementary material, figure S3*a*,*b*, *respectively*), scarlet ibis (*Eudocimus rubber*), helmeted guinea fowl (*Numida meleagris*), whitefaced owl (*Outs leucotis*) (electronic supplementary material, figure S4*a–c*, respectively), peregrine falcon (*Falco peregrinus*) and lanner falcon (*Falco biarmicus*, museum taxidermy specimen) (figure 2*e*,*f*, respectively).

The medulloid cells of the rachidial pith are distributed internal to the rachidial cortex (figure 5*a*,*c*) and comprise large, central gas-filled vacuoles. We show (electronic supplementary material, figure S6) that the

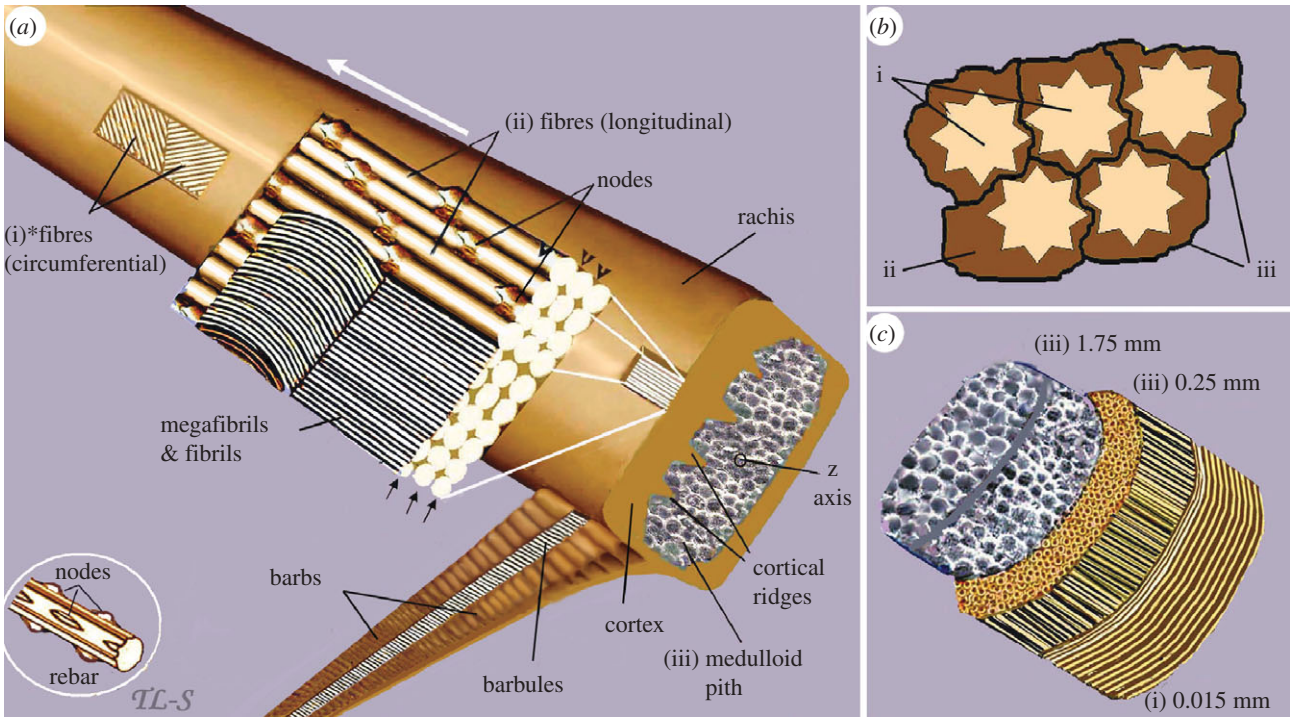

Figure 5. A schematic view of the three major structural components of the feather rachis. (*a*) (i) superficial layers of *fibres, the ultimate size-class in the hierarchy of feather keratin filaments (approx. 6 μm diameter), wound circumferentially round the rachis. (ii) The majority of the fibres extending parallel to the rachidial axis and through the depth of the cortex. Part of the section is peeled back to show why the fibres and even megafibrils are not usually recognized in histological sectioning, but rather only fibrils lower down the hierarchy (based on the electronic supplementary material, figure S2*c*). Any longitudinal section along the line of the arrows or at any point along the height of the fibre other than at the fibre surface (arrowheads) will fail to show the fibre. (iii) It shows the medulloid pith comprising gas-filled polyhedral structures (based on SEM images, electronic supplementary material, figures S5 and S6). Inset, part of a steel rebar with nodes, used in engineering technology to reinforce high-rise structures, analogous to rachidial fibres. (*b*) Schematic cross section of fibres and biodegraded 'matrix': (i) fibres; (ii) residual cytosol of keratinocytes presumably housing effete organelles and perhaps cytoskeletal elements—all degraded along with corneous envelope; (iii) interdigitating plasma membrane of the original keratinocytes with associated corneous envelope proteins. (*c*) A schematic three-dimensional cross section of the rachis showing approximate thickness (based on SEMs) of the three keratin layers comprising, (i) circumferential and (ii) longitudinal fibres of the cortex and (iii) polyhedra of medulloid pith. Asterisk denotes homologous with syncitial barbules.

multicellular mass of the medulloid pith still holds together and is tightly integrated with the cortex after 3 years biodegradation.

To summarize the results, the fibres of the feather rachis (i) are the thickest keratin filaments known (±6 μm); (ii) possess significantly thickened nodes (>25%) which (iii) occur near periodically, (iv) and are staggered in adjacent fibres; (v) occur predominantly axially but; (vi) include a small but important outer circumferential component; and (vii) are closely juxtaposed with the medulloid pith (electronic supplementary material, figure S6).

(b) *Phenotypic characterization of fungi—rRNA sequence analysis*

The genomic DNA analysis displayed 99 per cent sequence identity with the fungi *Alternaria arborescens*, *A. citri*, *A. alternata* and *A. tenuissima* (cf. Marcondes *et al.* 2008; other fungi and details in the electronic supplementary material, material and methods).

4. DISCUSSION

(a) *Morphology of β-keratogenic tissues of the feather*

Classical histological studies, recently enhanced by TEM analysis of barb differentiation, recognized three distinct cellular morphologies of β-keratogenic tissues of the feather (Alibardi 2007*a*,*b*): (i) a very flattened, proximo-distally (with reference to the feather) elongated form that characterizes the outer cortex (epicortex) of the rachis and of the barb rami (epitheloid cells)—not considered any further here; (ii) a cylindrical form, elongated proximo-distally, which characterizes the barbules and down feathers—syncitial barbule cells—the main focus here, and (iii) a polyhedral form, whose axes lack obvious spatial relation to feather axes, which characterizes the medulloid pith that is unique to the rachis and barb rami—mentioned here only functionally (Alibardi 2002; reviewed in Maderson *et al.* 2009).

(i) *Syncitial barbule cells of the feather rachis*

The heretofore known location of syncitial barbule cells is as barbules attached to barbs (Nitzsch 1867; Chandler 1916), which function to maintain vane integrity (figure 5*a*); barbules forming the plumulaceous (downy) portions of contour feathers (figure 4*b*); and barbules in embryonic down (Chandler 1916), which function to keep the barbs apart (Stettenheim 2000). The new location of syncitial barbules—in the feather rachidial cortex—had not been identified in 140+ years of study (Nitzsch 1867; Maderson 1972)—understandably

because it is the only instance where they occur not as free cells but tightly bonded with the keratin matrix. We shall refer to syncitial barbules when applied to their occurrence in the rachis, as fibres, a term that will better explain their structural and mechanical qualities; in all other cases, the term syncitial barbule prevails, bearing in mind their homology. The biological roles of the fibres are emergent properties of (i) tissue organization; (ii) increased relative mass at successive disto-proximal levels; and (iii) juxtapositioning to the medulloid tissues to which they adhere. Structurally, the importance of the fibres is implicit given that they form the bulk (approx. two-thirds) of the physical and chemical makeup of the rachis, as β-keratin bundles, and that flexural stiffness has been found to be largely controlled by the morphology of the cortical region (Purslow & Vincent 1978; Bonser 1996) (figure 5).

(b) *Biomechanical implications of the rachidial fibres (cortex)*

Both the newly emergent feather and the mature feather must transmit muscular force to undertake aerodynamic activity. The rachis of the feather can be regarded as a fibrous composite material, consisting of long fibres (contributing stiffness and strength) bonded by an amorphous matrix. Increased mass of fibres of the rachis in the thicker dorsal wall (also enhanced by cortical ridges; figure 5*a*, electronic supplementary material, figure S5, arrows), and proximally, give more distal portions of the feather greater flexibility. Feather shafts may be expected to buckle at lower bending moments *in vivo* (because of low tapering of rachis, i.e. high ratio of rachis height to diameter) than those measured in four-point bending (Corning & Biewener 1998). However, tight integration of the rachidial cortex with the medulloid pith (compact keratin (fibre–matrix texture) approximately 100 times stiffer than the medullary foam (Bonser 1996); figure 5*a*,*c*; electronic supplementary material, figures S5 and S6) may function to delay the onset of buckling under compressive loading by transference of tensile stresses from the cortical layer and absorption of the energy by the medulloid pith (Bonser 2001).

At present, we have little understanding regarding the nature of loads on the feather rachis during flight, apart from some uniaxial strain gauge measurements in the pigeon (Corning & Biewener 1998). We consider that predominant axial orientation of the fibres maximizes flexural rigidity while minimizing wing inertia and drag (Bonser & Purslow 1995; Cameron *et al.* 2003). It is equally possible that it is an adaptation to allow torsion of the asymmetric feather vane (Ennos 1995), because a composite with unidirectional fibres tends to have a lower torsional stiffness. This raises the question of the apparent lack of obvious keratinous cross-links for resisting excessive torsion. Crucially, we show fibres wound 8–10 fibres deep (approx. 15% of cortical depth) around the circumference of the rachidial cortex (approx. 60–70° to the rachidial long axis) (figure 3), directions consistent with X-ray diffraction analyses of fibrils (Astbury & Bell 1939; Earland *et al.* 1962; Busson *et al.* 1999). They indicate the presence of an anisotropic fibrous structure. Despite the relatively thin circumferential layer, we believe that it would be significant enough to control the hoop and longitudinal stresses (comparable to a thin-walled pressure cylinder) and prevent ovalization of the rachis.

Three characteristics of the fibres are of especial significance: (i) the highly thickened fibres, further enhanced by near-periodic thickened nodes (>25%, electronic supplementary material, table S2), may explain why measurements of cutting energies are approximately three times higher transversely than axially (Bonser *et al.* 2004); (ii) syncitial nodes are staggered in both two- and three-dimensional planes (figure 1; electronic supplementary material, figure S1), comparable to a 'brick and mortar' structure, increasing resistance to fracture, specifically the propagation of a crack (Ashby *et al.* 1995); and (iii) syncitial nodes function to prevent 'pull-out' of the fibres from the surrounding matrix and improve the transmission of forces, analogous in structure and function to steel rebars used in high-rise building construction (Santos *et al.* 2007; figure 5*a*, inset).

(c) *Developmental and evolutionary implications*

Although we anticipated a higher structural hierarchy of keratin filaments of the feather rachis than previously known, we could not have conceptualized that the discovery would involve syncitial barbule cells. Existing knowledge is of a basic mode of avian keratinization, i.e. columnar syncitial cells used in key feather structures—barbules in feather venation, barbules in the downy portions of contour feathers and barbules in embryonic down. Our study completes the picture with barbules as a major component of the rachidial cortex and, probably, the most critical usage—construction of a robust feather shaft. This remarkable variation in the usage of the syncitial barbule cells in both the embryonic and mature feather suggests that the material properties of feather keratin are constrained in an evolutionary sense by a highly conserved molecular structure of β keratins, considered a plesiomorphic feature of the archosaurian ancestor of crocodilians and birds (Sawyer & Knapp 2003), but nevertheless capable of forming diverse structural elements.

The present study raises as many questions as are answered. Incumbent on selective biodegradation was anticipation of a high sulphur content of the matrix, as shown in mammalian α keratins (Alexander & Earland 1950; Gillespie *et al.* 1968; Lindley & Cranston 1974). Selective biodegradation has certainly occurred and raises the question of the possible similarity of the β-keratin matrix of the feather with that of the α keratins of mammals, supporting recent proposals (reviewed in Bragulla & Homberger 2009) that the β keratins of sauropsid hard-cornified tissues resemble the non-filamentous KFAPs of mammals (i.e. 'matrix proteins'). Here, selective biodegradation of feather keratin suggests, as suspected (Bragulla & Homberger 2009) that the matrix and filamentous components of sauropsid hard cornified tissues have perhaps far less in common than previously thought and despite being tightly bonded together, retain distinctive chemical and molecular structures. Our use of microbial biodegradation as an investigative tool, although pioneering and considered 'clever' by two anonymous reviewers of this paper, which we gratefully acknowledge, was long overdue and, with fine-tuning (electronic supplementary material, material

and methods), may be used to investigate other cornified tissue, whose microstructures are notoriously difficult to study.

The study raises perhaps the most controversial question with respect to the evolution and developmental biology of the feather. Biomechanical reasons for syncitial barbules being incorporated in the feather rachis seem clear but, from an evolutionary perspective, pivotally—when did it happen? In feather evolution, the classical model is that feathers evolved from reptilian scales (Maderson 1972)—that a basic rachis would have formed first (with the potential for differentiation into other feather parts; Stettenheim 2000), then barbs and finally barbules. An alternative hypothesis is that barbs form first during development, and the rachis, a specialized form of fused barbs, appeared later as an evolutionary novelty (Prum 1999; Yu *et al.* 2002). This view has been closely linked with the contentious allegations of 'protofeathers' in the Chinese dinosaurs (e.g. Xu *et al.* 2001, 2009; Feduccia *et al.* 2005; Lingham-Soliar *et al.* 2007. Lingham-Soliar in press). The present discovery of barbules comprising the filamentous structure of the rachis adds a new key component to the controversial subject of feather evolution and raises important questions, which we hope will prove stimulating to both sides of the debate and, not least, in other aspects of feather structural and developmental biology.

T.L.-S. designed the study, conducted the experiments and analyses, and wrote the paper. R.H.C.B. aided biomechanical qualitative analyses of the findings. J.W.-S. provided technical support with respect to the electron microscopy.

We thank D. Allen (Durban Museum), Shaun Wilkinson (Umgeni Bird Park), Rob Armstrong (Rainbow Chickens) and T. Ganesen (UKZN) for birds used in the study and Evodia Setati (UKZN) for related microbiological work. A number of workers commented constructively on this manuscript, most notably Paul Maderson (City University of New York). We thank the anonymous reviewers for valued constructive comments and encouragement in publication.

REFERENCES

Alexander, P. & Earland, C. 1950 Structure of wool fibres. *Nature* **166**, 396–397. (doi:10.1038/166396a0)

Alibardi, L. 2002 Keratinization and lipogenesis in epidermal derivatives of the zebra finch *Taeniopygia guttata castanotis* (Aves, Passeriformes, Ploecidae) during embryonic development. *J. Morphol.* **251**, 294–308. (doi:10.1002/jmor.1090)

Alibardi, L. 2007*a* Cell organization of barb ridges in regenerating feathers of the quail: implications of the elongation of barb ridges for the evolution and diversification of feathers. *Acta Zool.* **88**, 101–117. (Stockholm). (doi:10.1111/j.1463-6395.2007.00257.x)

Alibardi, L. 2007*b* Wedge cells during regeneration of juvenile and adult feathers and their role in carving out the branching patterns of barbs. *Ann. Anat.* **189**, 234–242. (doi:10.1016/j.aanat.2006.11.008)

Ander, P. & Eriksson, E. 2008 Selective degradation of wood components by white-rot fungi. *Physiol. Plant.* **41**, 239–248. (doi:10.1111/j.1399-3054.1977.tb04877.x)

Ashby, M. F., Gibson, L. J., Wegst, U. & Olive, R. 1995 The Mechanical properties of natural materials. I. Material property charts. *Proc. Math. Phys. Sci.* **450**, 123–140. (doi:10.1098/rspa.1995.0075)

Astbury, W. T. & Bell, F. O. 1939 X-ray data on the structure of natural fibres and other bodies of high molecular weight. *Tabulae Biol.* **17**, 90–112.

Bonser, R. H. C. 1996 The mechanical properties of feather keratin. *J. Zool. Lond.* **239**, 477–484. (doi:10.1111/j.1469-7998.1996.tb05937.x)

Bonser, R. H. C. 2001 The mechanical performance of medullary foam from feathers. *J. Mater. Sci. Lett.* **20**, 941–942. (doi:10.1023/A:1010993219791)

Bonser, R. H. C. & Purslow, P. P. 1995 The Young's modulus of feather keratin. *J. Exp. Biol.* **198**, 1029–1033.

Bonser, R. H. C., Saker, L. & Jeronimidis, G. 2004 Toughness anisotropy of feather keratin. *J. Mater. Sci.* **39**, 2895–2896. (doi:10.1023/B:JMSC.0000021474.75864.ff)

Bragulla, H. H. & Homberger, D. G. 2009 Structure and functions of keratin proteins in simple, stratified, keratinized and cornified epithelia. *J. Anat.* **214**, 516–559. (doi:10.1111/j.1469-7580.2009.01066.x)

Busson, B., Engstrom, P. & Doucet, J. 1999 Existence of various structural zones in keratinous tissues revealed by X-ray microdiffraction. *J. Synchrotron Radiat.* **6**, 1021–1030. (doi:10.1107/S0909049599004537)

Cameron, G. J., Wess, T. J. & Bonser, R. H. C. 2003 Young's modulus varies with differential orientation of keratin in feathers. *J. Struct. Biol.* **143**, 118–123. (doi:10.1016/S1047-8477(03)00142-4)

Chandler, A. C. 1916 A study of the structure of feathers with reference to their taxonomic significance. *Univ. Calif. Publ. Zool.* **13**, 243–446.

Corning, W. R. & Biewener, A. A. 1998 *In vivo* strains in pigeon flight feather shafts: implications for structural design. *J. Exp. Biol.* **201**, 3057–3065.

Ennos, A. R. 1995 Mechanical behaviour in torsion of insect wings, blades of grass and other cambered structures. *Proc. R. Soc. Lond. B* **259**, 15–18. (doi:10.1098/rspb.1995.0003)

Deshmukh, S. K. 2004 Keratinophilic fungi on feathers of pigeon in Maharashtra, India. *Mycoses* **47**, 213–215. (doi:10.1111/j.1439-0507.2004.00983.x)

Dixit, A. K. & Kushwaha, R. K. S. 1991 Occurrence of keratinophilic fungi on Indian birds. *Folia Microbiol.* **36**, 383–386. (doi:10.1007/BF02814513)

Earland, C., Blakey, P. R. & Stell, J. G. P. 1962 Molecular orientation of some keratins. *Nature* **196**, 1287–1291. (doi:10.1038/1961287a0)

Eckhart, L. *et al.* 2008 Identification of reptilian genes encoding hair keratin-like proteins suggests a new scenario for the evolutionary origin of hair. *Proc. Natl Acad. Sci. USA* **105**, 18 419–18 423. (doi:10.1073/pnas.0805154105)

Feduccia, A., Lingham-Soliar, T. & Hinchcliffe, J. R. 2005 Do feathered dinosaurs exist? Testing the hypothesis on neontological and paleontological evidence. *J. Morphol.* **266**, 125–166. (doi:10.1002/jmor.10382)

Filshie, B. K. & Rogers, G. E. 1962 An electron microscope study of the fine structure of feather keratin. *J. Cell Biol.* **13**, 1–12. (doi:10.1083/jcb.13.1.1)

Fraser, R. D. B. & Parry, D. A. D. 2008 Molecular packing in the feather keratin filament. *J. Struct. Biol.* **162**, 1–13. (doi:10.1016/j.jsb.2008.01.011)

Fraser, R. D. B., MacRae, T. P., Parry, D. A. D. & Suzuki, E. 1971 The structure of feather keratin. *Polymer* **12**, 35–56. (doi:10.1016/0032-3861(71)90011-5)

Gillespie, J. M., Haylett, T. & Lindley, H. 1968 Evidence of homology in a high-sulphur protein fraction (SCMK-B2) of wool and hair α-keratins. *Biochem. J.* **110**, 193–200.

Kersten, P. & Cullen, D. 2007 Extracellular oxidative systems of the lignin-degrading Basidiomycete *Phanerochaete*

chrysosporium. *Fungal Genet. Biol.* **44**, 77–87. (doi:10.1016/j.fgb.2006.07.007)

Kushwaha, R. K. S. & Gupta, M. 2004 Diversity of keratinophilic fungi in soil and on birds. In *Microbiology and biotechnology for sustainable development* (ed. P. C. Jaic), pp. 59–70. New Delhi, India: CBS Publishers.

Lindley, H. & Cranston, R. W. 1974 The reactivity of the disulphide bonds of wool. *Biochem. J.* **139**, 515–523.

Lingham-Soliar, T. In press. Dinosaur protofeathers: pushing back the origin of feathers into the Middle Triassic? *J. Ornithol.* (doi:10.1007/s10336-009-0446-7)

Lingham-Soliar, T., Feduccia, A. & Wang, X. 2007 A new Chinese specimen indicates that 'protofeathers' in the Early Cretaceous theropod dinosaur *Sinosauropteryx* are degraded collagen fibers. *Proc. R. Soc. B.* **274**, 1823–1829. (doi:10.1098/rspb.2007.0352)

Lucas, A. M. & Stettenheim, P. R. 1972 *Avian anatomy—the integument*, vols 1 and 2. Washington, DC: U.S. Government Printing Office.

Maderson, P. F. A. 1972 On how an archosaurian scale might have given rise to an avian feather. *Am. Nat.* **176**, 424–428. (doi:10.1086/282783)

Maderson, P. F. A., Hillenius, W. J., Hiller, U. & Dove, C. C. 2009 Towards a comprehensive model of feather regeneration. *J. Morphol.* **270**, 1166–1208. (doi:10.1002/jmor.10747)

Marcondes, N. R., Taira, C. L., Vandresen, D. C., Svidzinski, T. I. E., Kadowaki, M. K. & Peralta, R. M. 2008 New feather-degrading filamentous fungi. *Microb. Ecol.* **56**, 13–17. (doi:10.1007/s00248-007-9319-x)

Martínez-Hernández, A. L., Velasco-Santos, C., de Icaza, M. & Castaño, V. M. 2005 Microstructural characterisation of keratin fibres from chicken feathers. *Int. J. Env. Pollut.* **23**, 162–178.

McKinnon, A. J. 2006 The self-assembly of keratin intermediate filaments into macrofibrils: is this process mediated by a mesophase? *Curr. Appl. Phys.* **6**, 375–378. (doi:10.1016/j.cap.2005.11.022)

Nitzsch, C. L. 1867 *Nitzsch's pterylography* (ed. P. L. Sclater). London, UK: Robert Hardwick for the Ray Society. (English translation by W. S. Dallas.)

Prum, R. O. 1999 The development and evolutionary origin of feathers. *J. Exp. Zool.* **285**, 291–306. (doi:10.1002/(SICI)1097-010X(19991215)285:4%3C291::AID-JEZ1%3E3.0.CO;2-9)

Purslow, P. P. & Vincent, J. F. V. 1978 Mechanical properties of primary feathers from the pigeon. *J. Exp. Biol.* **72**, 251–260.

Rudall, K. M. 1968 *Comprehensive biochemistry* (eds M. Florkin & E. H. Stotz), pp. 559–594. Amsterdam, The Netherlands: Elsevier.

Santos, P. M. D., Julio, E. N. B. S. & Silva, V. D. 2007 Correlation between concrete-to-concrete bond strength and the roughness of the substrate surface. *Constr. Build. Mater.* **21**, 1688–1695. (doi:10.1016/j.conbuildmat.2006.05.044)

Sawyer, R. H. & Knapp, L. W. 2003 Avian skin development and the evolutionary origin of feathers. *J. Exp. Zool. Mol. Dev. Evol.* **298B**, 57–72. (doi:10.1002/jez.b.26)

Stettenheim, P. R. 2000 The integumentary morphology of modern birds—an overview. *Amer. Zool.* **40**, 461–477. (doi:10.1093/icb/40.4.461).

Wainwright, S. A., Biggs, W. D., Currey, J. D. & Gosline, J. M. 1976 *Mechanical design in organisms*. London, UK: Edward Arnold.

Xu, X., Zhou, Z. & Prum, R. O. 2001 Branched integumental structures in *Sinornithosaurus* and the origin of birds. *Nature* **410**, 200–204. (doi:10.1038/35065589)

Xu, X., Zheng, X. & You, H. 2009 A new feather type in a nonavian theropod and the early evolution of feathers. *Proc. Natl Acad. Sci. USA* **106**, 832–634. See http://www.pnas.org_cgi_doi_10.1073/pnas.0810055106.

Yu, M., Wu, P., Widelitz, R. B. & Chuong, R. B. 2002 The morphogenesis of feathers. *Nature* **420**, 308. (doi:10.1038/nature01196)